Rotational excitation of AlH by Helium and Neon at low temperature: State-to-state inelastic cross section

ARTICLE *in* CHEMICAL PHYSICS LETTERS · MARCH 2014

Impact Factor: 1.9 · DOI: 10.1016/j.cplett.2014.03.028

4 AUTHORS, INCLUDING:

Jean Jules Fifen

University of Ngaoundere

25 PUBLICATIONS **96** CITATIONS

SEE PROFILE

Christophe Nkem

University of Douala

6 PUBLICATIONS **26** CITATIONS

SEE PROFILE

Mama Nsangou

University of Maroua

41 PUBLICATIONS **244** CITATIONS

SEE PROFILE

Chemical Physics Letters 600 (2014) 21–28

Contents lists available at ScienceDirect

Chemical Physics Letters

journal homepage: www.elsevier.com/locate/cplett

Rotational excitation of AlH by Helium and Neon at low temperature: State-to-state inelastic cross section

M. Pamboundom [a], J.J. Fifen [a], C. Nkem [b], M. Nsangou [a,c,*]

[a] Department of Physics, Faculty of Science, University of Ngaoundere, P.O. BOX 454 Ngaoundere, Cameroon
[b] Center for Atomic Molecular Physics and Quantum Optics, Faculty of Science, University of Douala, P.O. BOX 8580 Douala, Cameroon
[c] University of Maroua, ENS Maroua, P.O. BOX 46 Maroua, Cameroon

ARTICLE INFO

Article history:
Received 19 February 2014
In final form 12 March 2014
Available online 20 March 2014

ABSTRACT

In this work, inelastic rotational collisions of AlH with He and Ne were studied. The CCSD (T) method was used for the computation of accurate two dimensional potential energy surfaces (2-D-PESs). In the calculation of the 2-D-PESs, AlH was frozen at the experimental value of 3.1149 a_0. The recently published basis sets m-aug-cc-pV (Q+d) Z of Papajak and Truhlar, completed with bond functions placed at mid-distance between the center of mass of AlH and He/Ne atom for a better description of van der Waals interaction energy, was used throughout the computational process. The PESs of AlH–He and AlH–Ne were found to have global minima at (R = 6.9 a_0, θ = 68°) and (R = 6.9 a_0, θ = 69°) respectively, with corrresponding depths of 26.32 cm^{-1} and 48.70 cm^{-1}. These potentials were fitted analytically and expanded in terms of Legendre polynomials, then used for the evaluation of the integral cross sections of state-to-state rotational transitions in AlH induced by the collisions with He or Ne within the close coupling approach. The rate coefficients are computed for low kinetic temperatures ranging from 3 K to 300 K.

1. Introduction

A variety of molecules containing metallic elements have been observed in the circumstellar envelopes of late-type stars [1]. Metal cyanides, metal halides and oxides have been identified, such as NaCN [2,3], MgNC [4,3], SiCN [5], AlNC [6]. These observations have shown that aluminium appears to be the dominant metal in astrophysics with four such species (AlCl, AlF, AlNC and AlO) detected in either carbon- or oxygen-rich circumstellar material [1,6]. Moreover, the cosmic elemental of abundance of aluminium is 3×10^{-6}, as opposed to 4×10^{-5} for both silicon and magnesium [1,7]. Even though simple diatomic hydrides are the obvious choice of molecular metal carriers, such species have remain elusive in the interstellar medium (ISM). Halfen and Ziurys [1] stated that, the main problem in studying these molecules in interstellar and circumstellar environments is that their spectra occur in submillimeter and infrared wavelengths, where atmospheric transmission is poor. Aluminium hydride has attracted the interest of theoretical physico-chemists and spectroscopists, for many years [8–12]. The physico-chemical properties of this molecule has revealed its importance in nuclear engineering, in the preparation of electronically pure metal films, and in the purification of metals [11]. In astrophysics, AlH is of significant interest. It was found in the emission of sunspots [11,12] and atmospheres of M-, S-, Sp- and C-type stars [11,13].

Experimentally, the AlH molecule has been studied by electronic absorption or emission spectroscopy [10,11]. These authors have identified many bands in the visible and ultraviolet. The C-X band system of the AlH was also successively studied by Bengtsson [14], Grabe and Hulten [15], Khan [16] and Zhu et al. [17]. All these works aimed at the determination of precise values of the wavenumbers of lines, rotational terms values and improved molecular constants for the ground and excited states. The radiative and predissociated rotational levels lifetimes of AlH and AlD were measured by Baltayan and Nedelec [18]. More recently, the $J = 1 \leftarrow 0$ rotational transition was measured by Goto and Saito [19] and by Halfen and Ziurys [20]. Later, the $J = 2 \leftarrow 1$ and $J = 3 \leftarrow 2$ rotational transitions of AlD ($X^1\Sigma^+$) near 393 and 590 GHz were measured using submillimeter direct absorption spectroscopy [1]. By assuming that high deuterium enrichment occurs often in colder clouds, in particular for hydrides, because the low temperatures in the ISM heavily favor the formation of H_2D^+, Halfen and Ziurys [1] concluded that this ion may then exchange H to D in hydride species as follows:

$$H_2D^+ + AlH \rightarrow H_3^+ + AlD \quad (1)$$

* Corresponding author at: Department of Physics, ENS Maroua, University of Maroua, P.O. BOX 46 Maroua, Cameroon.
E-mail address: mnsangou@yahoo.com (M. Nsangou).

http://dx.doi.org/10.1016/j.cplett.2014.03.028
0009-2614/

Concerning the theoretical predictions on AlH, calculations have mainly been concentrated on the electronic structure of the ground state [9], the first low lying states [10,21] and the Rydberg states [8].

The interaction of diatomic or triatomic molecules with rare gas (or H, or H_2) are common interactions that take place in interstellar medium, circumstellar medium or in atmosphere. The computation of the inelastic rotational cross sections of the collision of such molecules with rare gas, hydrogen atom or hydrogen molecules has been subject of extensive studies by the teams of Alexander [22,23], Lique and Kłos [24]. The molecular systems resulting from such interactions also called van der Waals complexes are very important for the understanding of the structure and properties of gases, liquids as well as other systems. Many van der Waals hydride systems have been extensively studied during the last years, CH^+–He [25], MgH–He [27], NaH–He [28], LiH–Ne [29], LiH–Ar [30], NH/D–He [31]. Their accurate descriptions led to new insight into the behavior of atom–diatom collisions at various temperatures, and hence, to results of great interest to astrophysicists. Regarding the complexes of AlH with rare gases, it is worth mentioning that, to our knowledge, only the experimental and theoretical investigations on the AlH–Ar complex by the research group of Dagdigian in 1995 and 2000 [32–34], as well as the recent theoretical work by Pang et al. [35] were carried out. All the above clearly illustrate the importance of AlH in astrophysics and hence the effort devoted to conduct investigation on this molecular system.

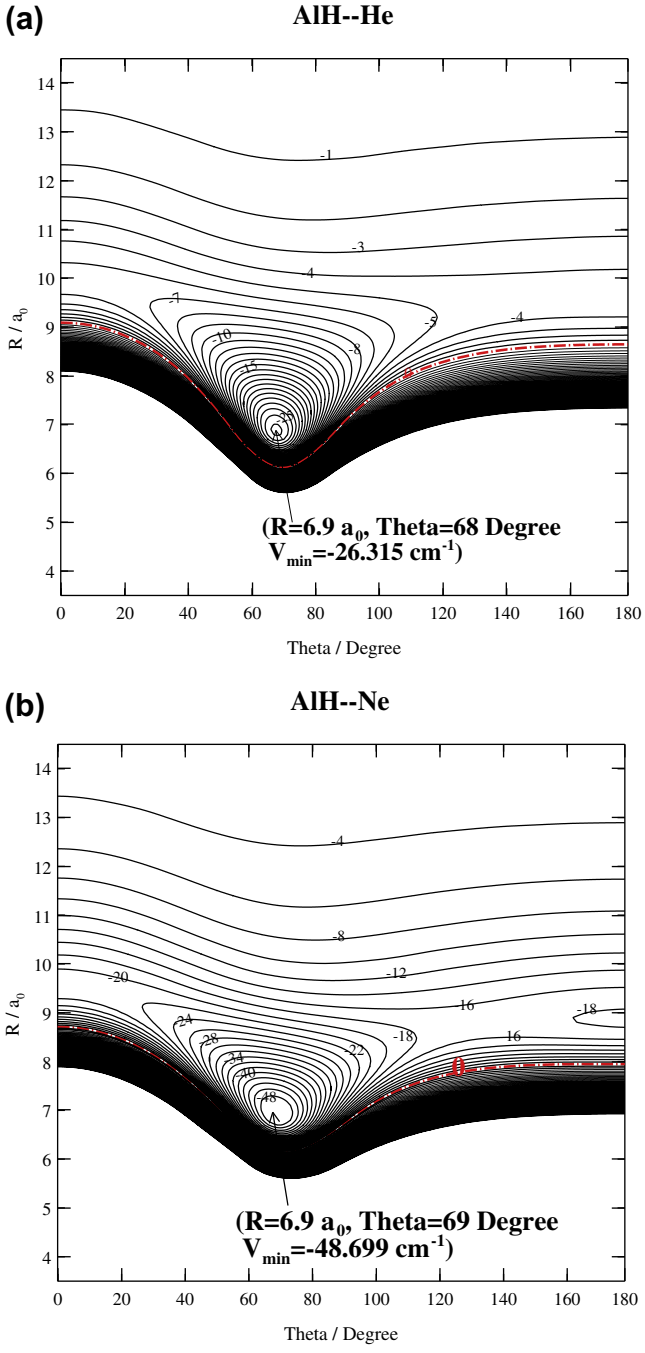

Figure 1. Potential energy surfaces of AlH–He (a) and AlH–Ne (b) as function of R and θ with AlH bond length frozen at $r_e = 3.1149\ a_0$. The energies are in cm^{-1}.

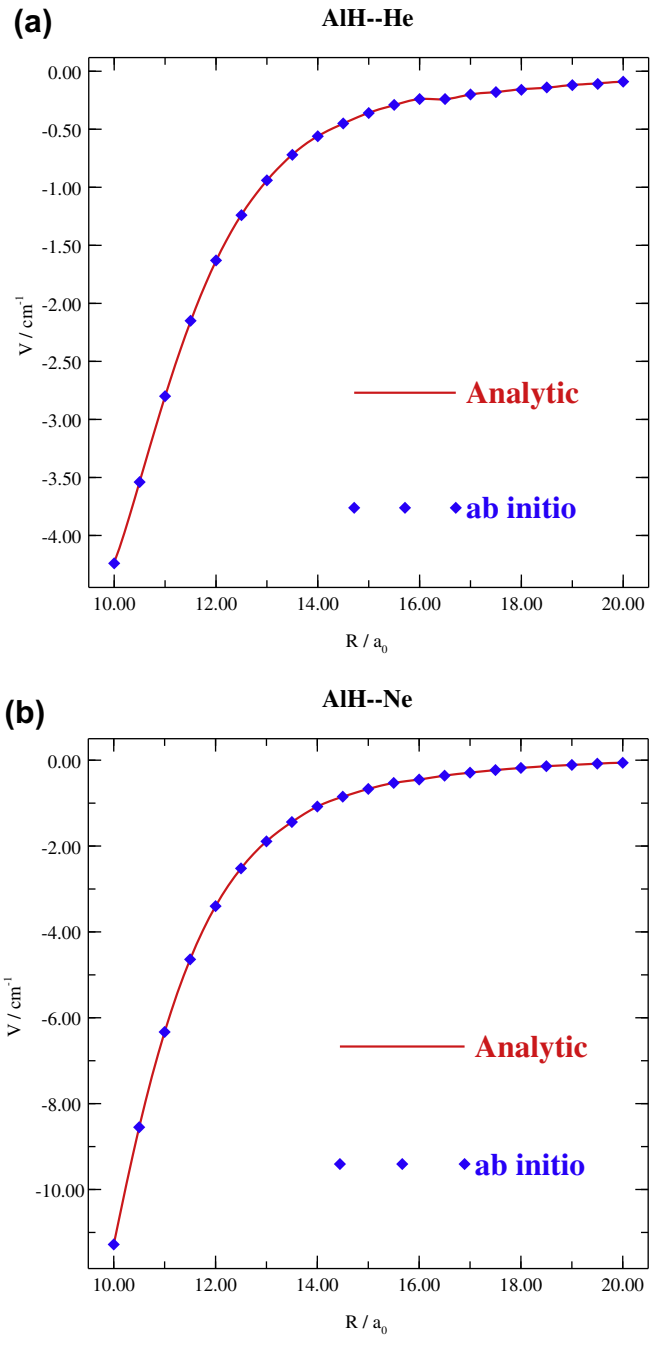

Figure 2. Comparison between the long-range ab initio and analytical potential energies for $\theta = 180^\circ$ for AlH–He (a) and AlH–Ne (b) complexes.

The present work deals with the calculations of the interaction energy of AlH ($X^1\Sigma^+$) with He and Ne atoms, and the rotational cross sections induced by these collisions. To the best of our knowledge, such parameters have not yet been reported in the literature.

2. Computational details and potential energy surfaces

The ab initio calculations were carried out using MOLPRO 2002 package [36]. The CCSD (T) method [37] was used thanks to the fact that the weight of the dominant configurations $(1a')^2(2a')^2(3a')^2(4a')^2(1a'')^2(5a')^2(6a')^2(7a')^2$ and $[core](6a')^2(7a')^2(8a')^2(9a')^2(10a')^2(2a'')^2$ respectively for AlH–He and AlH–Ne complexes were greater than 0.95. The basis sets associated with the CCSD (T) method was the modified augmented correlation consistent valence polarized quadruple zeta, maug-cc-pV (Q+d) Z recently published by Papajak and Truhlar [38]. To this basis we have added an additional (3*s*2*p*2*d*1*f*) set of midbond functions. The exponent of these midbond functions are 0.9, 0.6, 0.1 for the *s* functions, 0.60, 0.20 for *p* and *d* functions, and 0.3 for *f* function [39]. These midbond functions have been proven to be very efficient for correct description of the intersystem correlation interaction energy, specially for van der Waals systems [25,40]. To correct the basis set superposition error (BSSE) at all the geometries, the counterpoise procedure of Boys and Bernadi [41] was used. As a result, the interaction energy is given by

$$V(r = r_e, R, \theta) = E_{\mathrm{AlH-He/Ne}}(R, \theta) - E_{\mathrm{AlH}}(R, \theta) - E_{\mathrm{He/Ne}}(R, \theta). \quad (2)$$

As shown by previous authors [30,42], the 2-D-potential energy surface (2-D-PES) calculated at the frozen equilibrium r-distance and the full 3-D-PES averaged over the ground state are very similar. This means that the use of a rigid body 2-D-PES is sufficient when the calculations are limited to the lowest vibrational level. Therefore, for AlH ($X^1\Sigma^+$)–He (^{1}S) or AlH ($X^1\Sigma^+$)–Ne (^{1}S) the AlH is frozen at the experimental equilibrium geometry of the $X^1\Sigma^+$ ground state, i.e. 3.1149 a_0. The interaction 2-D-PES for the above-mentioned van der Waals complexes were computed in the conventional Jacobi coordinate system ($r = r_e, R, \theta$). Here r_e is AlH bond length. *R* refers to the distance between the He or Ne atom and the center of mass (CM) of AlH, and θ is the angle between the vector **R** and the AlH molecular axis. The collinear axis (AlH–He/Ne) corresponds to $\theta = 0°$.

Throughout the computation of the 2-D-PES, the values of the radial coordinate *R* were chosen from 4.0 to 20 bohr in a uniform step of 0.5 bohr. The angle θ was assigned the values from 0° to 180° with a uniform step size of 10°. Furthermore, an interpolation of the grid was done with steps of 1° for θ and 0.1 a_0 for *R*. Figure 1 displays the contour plots of our PES's. We note a strong anisotropy of both surfaces. These contour plots show that for the AlH–He complex, the global minimum of 26.315 cm^{-1} is located at $R = 6.9$ a_0 and $\theta = 68°$, while for the AlH–Ne complex, the global minimum of depth 48.699 cm^{-1} occurs at $R = 6.9$ a_0 and $\theta = 69°$. Compared with the previous theoretical work by Pang et al., we note a good agreement since the difference between the depth of our global minimum and that calculated by these authors at the CCSD (T)/aV5Z level is only 2.63 cm^{-1}. The shape of these surfaces are similar with those of the $CH^+(X^1\Sigma^+)$–He (^{1}S)[25], $SiH^+(X^1\Sigma^+)$–He (^{1}S)[26], MgNC($X^1\Sigma^+$)–He (^{1}S) or AlNC($X^1\Sigma^+$)–He (^{1}S)[3] systems, which are almost T-shape. It could also be noted after the analysis of the cuts of the PES that both collinear geometries at $\theta = 0°$ (i.e. AlH–He/Ne) or $\theta = 180°$ (i.e. He/Ne–AlH) are local minima. For the AlH–He complex, the depth of both minima are 6.402 cm^{-1} and 4.492 cm^{-1} and they are located respectively at ($\theta = 0°$, $R = 9.9$ bohr), and ($\theta = 180°$, $R = 9.6$ bohr). For the AlH–Ne complex, these local minima occur at $R = 9.6$ a_0 and 8.9 a_0 respectively for $\theta = 0°$ and $\theta = 180°$, and the corresponding depths are 19.155 cm^{-1} and 16.323 cm^{-1}. Finally, it is worth mentioning from both collinear collisions that, attraction is more stronger for $\theta = 0°$, i.e. approach for He (or Ne) towards H atom. This strength increases when He atom is substituted by Ne atom. Moreover, it should also be noted that for the overall minima, those for AlH–Ne complex are deeper than those of the AlH–He complex. This may be explained by the fact that Ne atom polarises AlH molecule more than He atom.

In order to perform the scattering calculations, the 2-D-PESs were fitted using the procedure of Werner et al. [24,25,43]. We have performed separate fits of the potential energies vs. angle, for each value of *R*. This was done by projections using quadrature and expanded in terms of the Legendre polynomials as

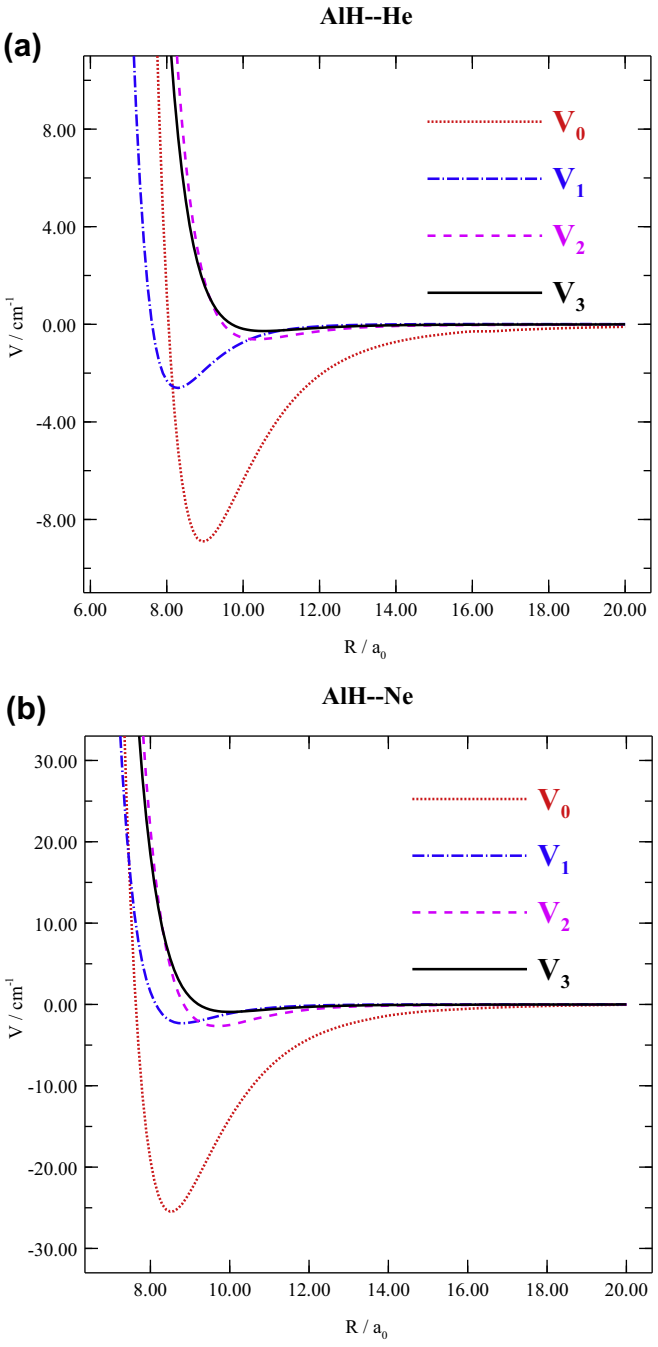

Figure 3. V_λ expansions of the interaction potential energy surface ($\lambda = 0, 1, 2, 3$) for AlH–He (a) and AlH–Ne (b) complexes as a function of the Jacobi coordinate *R*.

Table 1
Some selected rotational cross sections (in Å^2) of AlH in its collision with He or Ne as functions of J_{max} for different energies.

Energy	Transition	J_{max} = 10	J_{max} = 12	J_{max} = 15	J_{max} = 16	J_{max} = 23	J_{max} = 24
AlH–He							
100 cm^{-1}	0→1	1.083	1.083	1.083	1.083	1.083	1.083
	0→2	3.839	3.839	3.839	3.839	3.839	3.839
	1→2	2.188	2.188	2.188	2.188	2.188	2.188
	2→3	2.144	2.144	2.144	2.144	2.144	2.144
400 cm^{-1}	0→1	1.699	1.699	1.699	1.699	1.699	1.699
	0→2	3.887	3.887	3.887	3.887	3.887	3.887
	1→2	2.668	2.668	2.668	2.668	2.668	2.668
	2→3	3.031	3.031	3.031	3.031	3.031	3.031
	5→6	2.179	2.178	2.178	2.178	2.178	2.178
	5→7	0.697	0.698	0.698	0.698	0.698	0.698
	6→7	1.238	1.238	1.238	1.238	1.238	1.238
900 cm^{-1}	0→1	1.363	1.364	1.364	1.364	1.364	1.364
	0→2	3.111	3.110	3.111	3.111	3.111	3.111
	1→2	2.697	2.684	2.684	2.684	2.684	2.684
	2→3	3.096	3.097	3.097	3.097	3.097	3.097
	5→6	3.194	3.179	3.179	3.179	3.179	3.179
	5→7	4.387	4.384	4.384	4.384	4.384	4.384
	5→8	0.905	0.900	0.899	0.899	0.899	0.899
	6→7	3.182	3.145	3.147	3.147	3.147	3.147
	8→9	2.971	3.037	3.024	3.024	3.024	3.024
	8→10	0.824	0.904	0.924	0.924	0.924	0.924
	9→10	3.618	2.330	2.356	2.356	2.356	2.356
1500 cm^{-1}	0→1	1.045	1.052	1.049	1.049	1.049	1.049
	0→2	2.518	2.501	2.503	2.503	2.503	2.503
	1→2	2.389	2.342	2.342	2.342	2.342	2.342
	2→3	2.837	2.774	2.788	2.788	2.788	2.788
	5→6	3.066	3.058	3.047	3.047	3.047	3.047
	5→7	5.607	5.535	5.486	5.485	5.485	5.485
	5→8	1.286	1.086	1.096	1.097	1.097	1.097
	6→7	3.221	3.063	3.077	3.078	3.078	3.078
	8→9	3.027	3.296	3.201	3.200	3.200	3.200
	8→10	2.859	3.159	3.236	3.236	3.236	3.236
	9→10	7.038	3.441	3.332	3.333	3.333	3.333
2000 cm^{-1}	0→1	0.923	0.910	0.905	0.905	0.905	0.905
	0→2	2.240	2.244	2.239	2.239	2.239	2.239
	1→2	2.119	2.096	2.084	2.085	2.084	2.084
	2→3	2.710	2.534	2.565	2.568	2.568	2.568
	5→6	2.958	2.908	2.874	2.873	2.872	2.872
	5→7	5.801	5.430	5.320	5.318	5.318	5.318
	5→8	1.437	1.203	1.212	1.216	1.215	1.215
	6→7	3.100	2.946	2.914	2.919	2.917	2.917
	8→9	3.170	3.192	3.056	3.047	3.049	3.049
	8→10	3.682	4.361	4.452	4.456	4.456	4.456
	9→10	7.151	3.423	3.150	3.150	3.148	3.148
2500 cm^{-1}	0→1	0.854	0.845	0.828	0.829	0.828	0.828
	0→2	2.133	2.129	2.122	2.118	2.119	2.119
	1→2	1.907	1.886	1.860	1.863	1.862	1.862
	2→3	2.503	2.386	2.373	2.379	2.379	2.379
	5→6	2.985	2.736	2.709	2.709	2.707	2.707
	5→7	5.695	5.143	4.963	4.959	4.959	4.959
	5→8	1.476	1.354	1.320	1.328	1.326	1.326
	6→7	2.960	2.895	2.764	2.771	2.766	2.766
	8→9	3.318	3.085	2.914	2.886	2.892	2.892
	8→10	4.064	5.050	4.891	4.890	4.867	4.867
	9→10	7.098	3.305	2.996	2.989	2.982	2.982
AlH–Ne							
100 cm^{-1}	0→1	1.614	1.614	1.614	1.614	1.614	1.614
	0→2	4.817	4.817	4.817	4.817	4.817	4.817
	0→3	0.612	0.612	0.612	0.612	0.612	0.612
	1→2	2.701	2.701	2.701	2.701	2.701	2.701
	1→3	2.801	2.801	2.801	2.801	2.801	2.801
	2→3	6.804	6.804	6.804	6.804	6.804	6.804
900 cm^{-1}	0→1	0.949	0.948	0.948	0.948	0.948	0.948
	0→2	3.793	3.795	3.795	3.795	3.795	3.795
	1→2	2.184	2.183	2.183	2.183	2.183	2.183
	2→3	2.578	2.573	2.574	2.574	2.574	2.574
	5→6	4.824	4.766	4.766	4.766	4.766	4.766
	5→7	1.763	1.802	1.803	1.803	1.803	1.803
	6→7	5.338	5.391	5.388	5.388	5.388	5.388
	8→9	4.534	4.979	4.966	4.966	4.966	4.966
	8→10	0.824	0.995	1.006	1.006	1.006	1.006
	9→10	3.980	3.465	3.489	3.489	3.489	3.489
1500 cm^{-1}	0→1	0.749	0.743	0.744	0.745	0.745	0.745

Table 1 (*continued*)

Energy	Transition	J_{max} = 10	J_{max} = 12	J_{max} = 15	J_{max} = 16	J_{max} = 23	J_{max} = 24
	0→2	3.405	3.398	3.396	3.396	3.396	3.396
	1→2	1.698	1.676	1.676	1.676	1.676	1.676
	2→3	2.300	2.289	2.291	2.291	2.291	2.291
	5→6	3.875	3.693	3.688	3.688	3.688	3.688
	5→7	2.714	2.873	2.885	2.885	2.885	2.885
	6→7	4.702	4.509	4.488	4.488	4.488	4.488
	8→9	6.038	5.393	5.444	5.445	5.444	5.444
	8→10	1.844	2.091	1.968	1.968	1.968	1.968
	9→10	6.958	5.994	5.502	5.500	5.500	5.500
2000 cm^{-1}	0→1	0.682	0.676	0.672	0.672	0.672	0.672
	0→2	3.261	3.227	3.229	3.229	3.229	3.229
	1→2	1.438	1.424	1.421	1.420	1.420	1.420
	2→3	2.050	2.029	2.012	2.013	2.012	2.012
	5→6	3.342	3.167	3.104	3.101	3.101	3.101
	5→7	3.701	3.984	3.999	4.001	4.001	4.001
	6→7	4.228	3.863	3.812	3.814	3.814	3.814
	8→9	5.606	5.173	5.072	5.064	5.067	5.067
	8→10	2.662	2.202	1.936	1.929	1.928	1.928
	9→10	8.613	6.014	5.379	5.391	5.384	5.384
2500 cm^{-1}	0→1	0.655	0.620	0.620	0.620	0.620	0.620
	0→2	3.060	3.051	3.043	3.042	3.041	3.041
	1→2	1.315	1.272	1.271	1.268	1.269	1.269
	2→3	1.882	1.792	1.770	1.766	1.767	1.767
	5→6	2.960	2.781	2.712	2.712	2.710	2.710
	5→7	4.451	4.747	4.748	4.735	4.737	4.737
	6→7	3.852	3.414	3.300	3.288	3.285	3.285
	8→9	5.373	4.863	4.588	4.574	4.560	4.560
	8→10	2.974	2.416	2.188	2.187	2.183	2.183
	9→10	9.024	5.913	5.086	5.043	5.041	5.041

$$V(r = r_e, R, \theta) = \sum_{\lambda=0}^{\lambda_{max}} V_\lambda(R) P_\lambda(cos(\theta)), \quad (3)$$

where λ varies from 0 to 18. The comparison between the long-range ab initio and analytical potential energies for $\theta = 180^\circ$ are presented in Figure 2. Figure 3 gives the first four terms of V_λ respectively for AlH-He and AlH-Ne complexes. Based on the results coming out from Figure 1 to Figure 3, one concludes on one hand that, the values of R provide sufficiently repulsive potentials for all orientations, and on the other hand that, our scattering calculations may be performed with confidence for $R \geqslant 4.0\ a_0$. Furthermore, on the entire grid, the average relative difference between ab initio calculations and analytic fit is lower than 1 percent.

3. Scattering calculations

3.1. Cross sections

The calculations of the state-to-state rotational excitation cross sections induced by the collisions of AlH by He or Ne were performed using the MOLSCAT code [44]. This program which is based on the quantum mechanical Close Coupling (CC) approach developed by Arthurs and Dalgarno [45] enabled the computation for values of J ranging from 0 to 19 and a total energy up to 2500 cm^{-1} for AlH–He and AlH–Ne complexes.

For $E \leq 100\ cm^{-1}$, the energy step was set to 0.1 cm^{-1}; from 100 cm^{-1} to 200 cm^{-1} it was set to 0.2 cm^{-1}; from 200 cm^{-1} to 450 cm^{-1} it was set to 0.5 cm^{-1}; 1.0 cm^{-1} from 450 cm^{-1} to 700 cm^{-1}; 5 cm^{-1} from 700 cm^{-1} to 900 cm^{-1}; 10 cm^{-1} from 900 cm^{-1} to 1000 cm^{-1}; 50 cm^{-1} from 1000 cm^{-1} to 1500 cm^{-1}; 75 cm^{-1} from 1500 cm^{-1} to 2000 cm^{-1}; and finally set to 100 cm^{-1} from 2000 cm^{-1} to 2500 cm^{-1}.

It is worth mentioning that at a collision energy of 1000 cm^{-1}, J = 13 is closed (See Supplementary materials; Table 1). The rotational basis sets used for AlH–He are J_{max}=10 when E$\leqslant$450 cm^{-1}, J_{max} = 15 when 450 $cm^{-1} \leqslant E <$ 700 cm^{-1}, J_{max}=16 for 700 $cm^{-1} \leqslant E <$ 1000 cm^{-1}, J_{max} = 23 for 1000 $cm^{-1} \leqslant E <$ 2400 cm^{-1}, and J_{max} = 24 for 2500 cm^{-1}. The rotational basis sets are the same for AlH–Ne. These values come from a series of convergence tests reported in Table 1. They correspond to the best values for a good accuracy of the computed cross sections. For integration, we have fixed the steps as follows, for E $\leqslant$ 450 cm^{-1} STEPS = 20, for 450 < E $\leqslant$ 2500 cm^{-1} STEPS = 10.

The other parameters required by MOLSCAT can be seen in Supplementary materials (Table 2). These parameters were fixed in the program after the above-mentioned convergence tests. The maximum value of the total angular momentum J_{tot} was appropriately chosen to ensure the convergence of the cross section within 0.01 $Å^2$ for diagonal terms and 0.001 $Å^2$ for off-diagonal terms. Some values of J_{tot} are given in Supplementary materials (Table 3). The coupled equations were solved using the improved log derivative propagator for inelastic scattering of Manolopoulos [46].

Figures 4 and 5 display the collisional excitation cross sections of AlH by He and by Ne as function of the kinetic energy E. Panel (a) of these figures give transitions from the first level, while panel (b) stands for $\Delta J = 2$. The figures illustrating $\Delta J = 1$ for AlH–He and AlH–Ne are given in Supplementary materials (Figures 1 and 2). These cross sections present some resonances. Moreover, these resonances are more important for AlH-Ne because the global minimum for AlH–Ne is deeper, and may also be explained, on one hand by the presence of quasi-bound states arising from tunneling through the centrifugal barrier (shape resonances), and on the other hand by the presence of an attractive well around $\theta = 68^\circ$ (or 69°) that allows He (or Ne) atom to be temporarily trapped into the well, enabling the formation of quasi-bound states before the dissociation of the complex (Feshbach resonances) [47,48].

It is also worth mentioning that the magnitude of the cross sections for 0⟶2 transition is greater than other transitions. This is confirmed by Figures 4 and 5. In panel (a) of these figures, we note for the transitions 0⟶1 and 0⟶2 that, for kinetic energies less than ~600 cm^{-1} the magnitude of the cross section are the greatest for both transitions, while for the kinetic energies greater than ~600 cm^{-1}, the transitions 0⟶4 and 0⟶2 are the greatest,

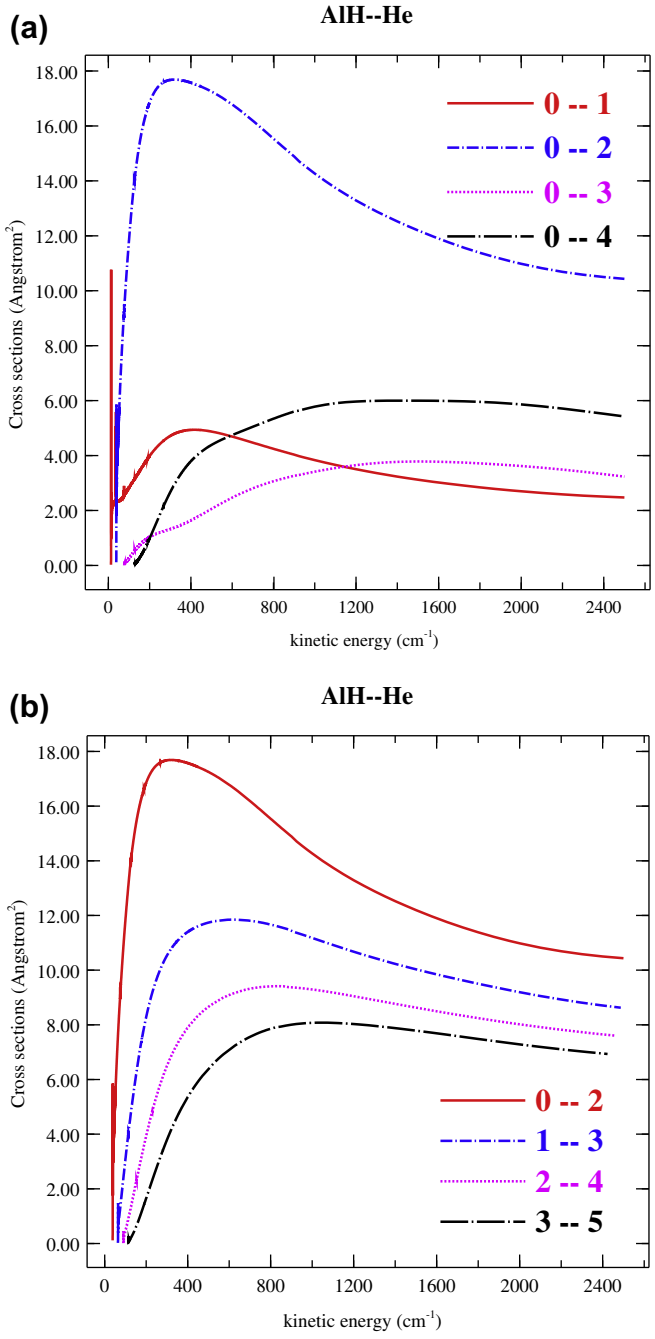

Figure 4. Collisional excitation cross sections of AlH by He from the first level (a) and $\Delta J = 2$ (b) as a function of the kinetic energy.

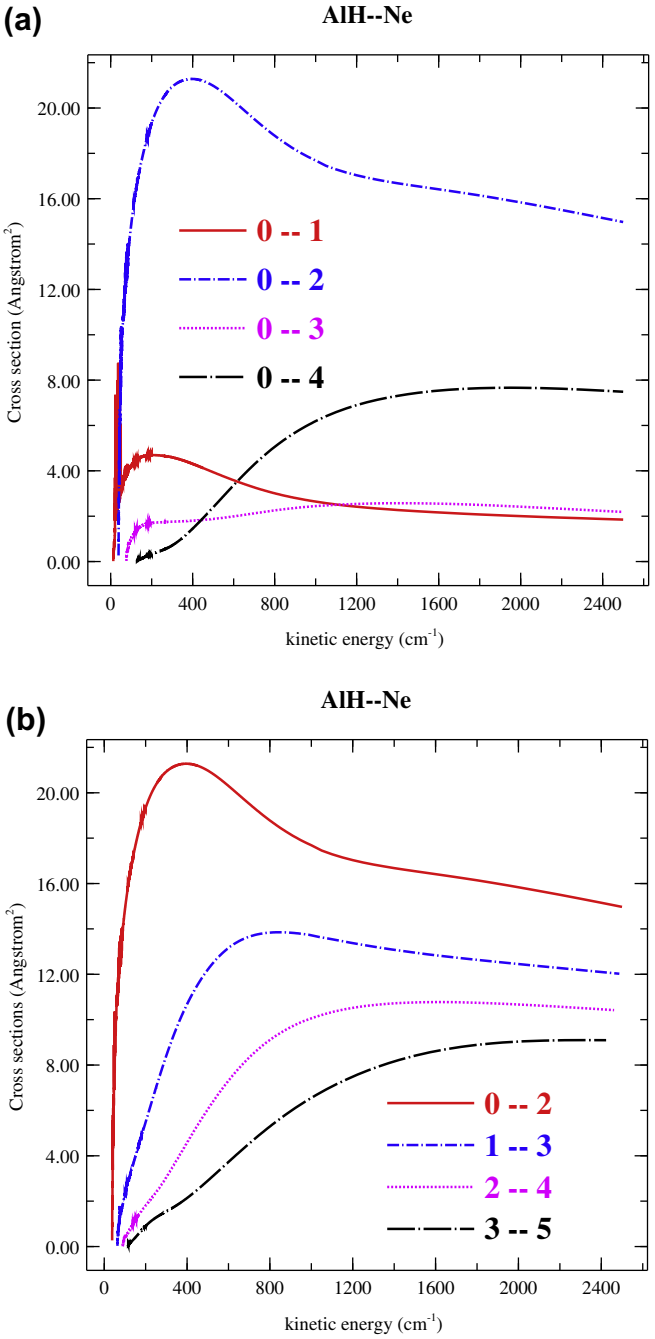

Figure 5. Collisional excitation cross sections of AlH by Ne from the first level (a) and $\Delta J = 2$ (b) as a function of the kinetic energy.

confirming the propensity towards even ΔJ transitions. The transitions $0 \longrightarrow 2$ and $1 \longrightarrow 3$ remain the most important for a wide range of the kinetic energy (see Figure 6 for AlH–He, (or Supplementary materials, Figure 3 for AlH–Ne)). The propensity seen in favor of even ΔJ transitions are due to the shape of the PESs which have near-homonuclear symmetry. In addition, this result is similar to that obtained recently by Hern′andez et al. [3] in the case of MgCN–He complex.

3.2. Collisional rates

The upward and downward rate coefficients are computed by convolving the collision cross sections $\sigma_{J \longrightarrow J'}$ with a Maxwell–Boltzmann distribution of kinetic energies,

$$q_{J \longrightarrow J'}(T) = \left(\frac{8\beta^3}{\pi\mu}\right)^{1/2} \int_0^\infty E\sigma_{J \longrightarrow J'}(E_T) e^{-\beta E} dE. \quad (4)$$

where T is the kinetic temperature, μ is the reduced mass of the complex (3.50183 a.u. for AlH–He and 11.72573 a.u. for AlH–Ne), $\beta = 1/k_B T$, k_B the Boltzmann constant and $E = E_T - E_J$ is the relative kinetic energy and E_T the total energy. The rate coefficients computed for low kinetic temperatures ranging from 3 K to 300 K are given as Supplementary materials. Figure 7 illustrates the variation of the upward collisional rates with some selected kinetic temperatures respectively for AlH–He and AlH–Ne complexes. Both subfigures show that the collisional rates exhibit the same trend as already observed for the cross sections, i.e. the propensity towards

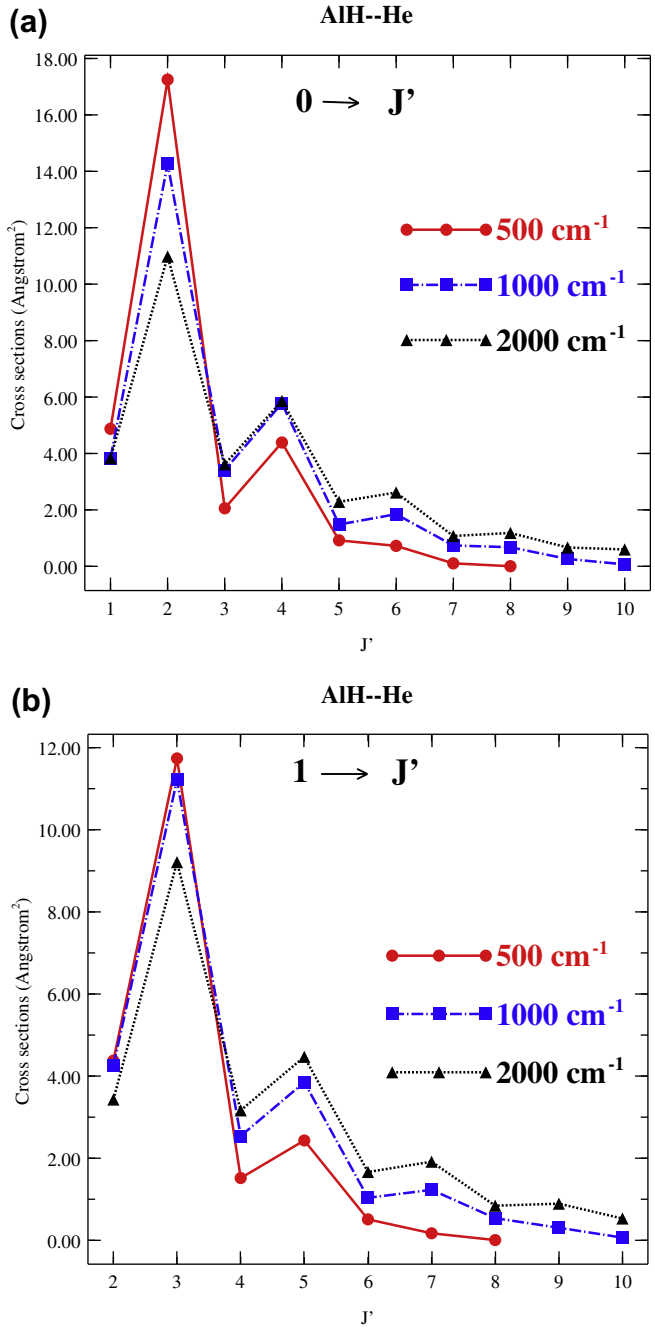

Figure 6. Collisional excitation cross sections of AlH by He as functions of J for some selected values of the Kinetic Energy.

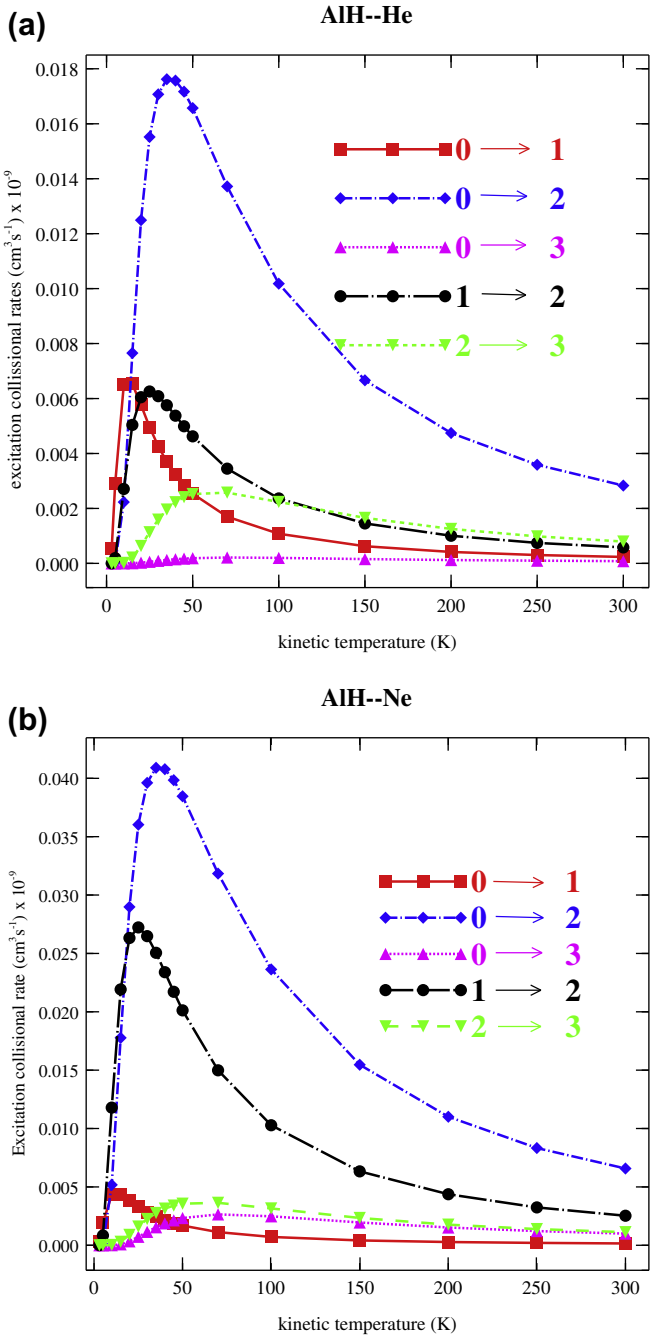

Figure 7. Upward collisional rates for AlH–He complex (a), and for AlH–Ne complex (b) as a function of the kinetic temperatures.

even ΔJ transitions. One notices that the collisional rates increase rapidly in some cases and decrease smoothly with the kinetic temperature.

4. Conclusions

In the present work, we have carried out an ab initio computation of the 2D-PES for the AlH–He and AlH–Ne complexes. These calculations were done at the CCSD (T) level of theory associated with the recently published basis sets m-aug-pV (Q+d) Z of Papajak and Truhlar. The shape of the 2D-PES was found to be close to those of the $CH^+(X^1\Sigma^+)$–He (^{1}S), $SiH^+(X^1\Sigma^+)$–He (^{1}S), MgCN($X^1\Sigma^+$)–He (^{1}S) or AlNC($X^1\Sigma^+$)–He (^{1}S) systems, which are almost T-shape. Then, the full quantum mechanical Close Coupling method was used to determine the state-to-state rotational excitation cross sections. By convolving these cross sections with a Maxwell–Boltzmann distribution of kinetic energies, we have derived rotational rate coefficients. From this study, we found that the 0⟶2 transition is dominant. Furthermore, other parameters presented in this work, notably collisional rates, may be useful for future astrosphysical investigations.

Acknowledgements

The authors would like to thank K. Hammami, D. Ben Abdallah and N. Jaidane of the laboratory LSAMA (University Tunis El Manar,

Tunis, Tunisia) and L.C. Owono Owono of the Higher Teachers' Training College (University of Yaounde I, Yaounde, Cameroon) for their helpful comments. They also thank the reviewers for their valuable remarks.

Appendix A. Supplementary data

Supplementary data associated with this article can be found, in the online version, at http://dx.doi.org/10.1016/j.cplett.2014.03.028.

References

[1] D.T. Halfen, L.M. Ziurys, Astrophys. J. 713 (2010) 520.
[2] B.E. Turner, T.C. Steimle, L. Meerts, Astrophys. J. 426 (1994) L97.
[3] M. Hernández Vera, F. Lique, F. Dumouchel, J. Kłos, J. Rubayo Soneira, M.-L. Senent, MNRAS 432 (2013) 468.
[4] L.M. Ziurys, A.J. Apponi, M. Guélin, J. Cernicharo, Astrophys. J. 445 (1995) L47.
[5] M. Guélin, S. Muller, J. Cernicharo, J. Apponi, C.A. Gottlieb, M.C. McCarthy, P. Thaddeus, Astron. Astrophys. 363 (2000) L9.
[6] L.M. Ziurys, C.S. Savage, J.L. Highberger, A.J. Apponi, M. Guélin, J. Cernicharo, Astrophys. J. 564 (2002) L45.
[7] N. Grevesse, A.J. Sauval, Space Sci. Rev. 85 (1998) 161.
[8] F. Grimaldi, A. Lacourt, H. Lefebvre-Brion, C.M. Moser, J. Mol. Spectrosc. 20 (1966) 341.
[9] P. Pyykko, J.P. Desclaux, Chem. Phys. Lett. 42 (1976) 545.
[10] M.O. Matos, B.O. Roos, A.J. Sadlej, G.H.F. Diercksen, Chem. Phys. 119 (1988) 71.
[11] W. Szajna, M. Zachwieja, J. Mol. Spectrosc. 260 (2010) 130.
[12] B. Karthikeyan, S.P. Bagare, F. Rajamanickam, V. Raja, Solar Phys. 264 (2010) 279.
[13] C. Herbig, Publ. Astron. Soc. Pac. 68 (1956) 204.
[14] E. Bengtsson, Z. Phys. 51 (1928) 889.
[15] B. Grabe, E. Hulten, Z. Phys. 114 (1939) 470.
[16] M.A. Khan, Proc. Phys. Soc. 71 (1958) 65.
[17] Y. Zhu, R. Shehadeh, E. Grant, J. Chem. Phys. 97 (1992) 883.
[18] P. Baltayan, O. Nedelec, J. Chem. Phys. 70 (1979) 2399.
[19] M. Goto, S. Saito, ApJ 452 (1995) L147.
[20] D.T. Halfen, L.M. Ziurys, ApJ 607 (2004) L63.
[21] M. Pelissier, J.P. Malrieu, J. Chem. Phys. 67 (1977) 5963.
[22] K.B. Gubbels et al., J. Chem. Phys. 136 (2012) 144308.
[23] H. Chadwick et al., J. Chem. Phys. 137 (2012) 154305.
[24] Y. Kalugina, J. Kłos, F. Lique, J. Chem. Phys. 139 (2013) 074301.
[25] K. Hammami, L.C. Owono Owono, N. Jaidane, Z. Ben Lakhdar, J. Mol. Struct. (theochem) 853 (2008) 18.
[26] C. Nkem, K. Hammami, A. Manga, L.C. Owono Owono, N. Jaidane, Z. Ben Lakhdar, J. Mol. Struct. Theochem 901 (2009) 220.
[27] X. Xu, M. Niu, X. Chen, X. Hu, W. Huang, E. Feng, Comput. Theor. Chem. 964 (2011) 49.
[28] B.K. Taylor, J. Chem. Phys. 121 (2004) 7725.
[29] Y. Lu, D. Xie, M. Yang, G. Yan, Chem. Phys. Lett. 327 (2000) 305.
[30] A. Niane, K. Hammami, N.A. Boye Faye, N. Jaidane, Comput. Theor. Chem. 993 (2012) 20.
[31] F. Dumouchel, J. Kłos, R. Toboła, A. Bacmann, S. Maret, P. Hily-Blant, A. Faure, F. Lique, J. Chem. Phys. 137 (2012) 114306.
[32] M. Yang, M.H. Alexander, S. Gregurick, P.J. Dagdigian, J. Chem. Phys. 102 (1995) 2413.
[33] E. Hwang, P.J. Dagdigian, J. Chem. Phys. 106 (1995) 2426.
[34] B. Nizamov, P.J. Dagdigian, J. Chem. Phys. 113 (2000) 4124.
[35] L.-J. Pang, R.-K. Wang, Y. Wang, J. Guangxi Normal University (Natural Science Edition), 31 (2013) 6.
[36] MOLPRO, a package of ab initio programs designed by H.-J. Werner and P.J. Knowles, version 2002.1, R.D. Amos, A. Bernhardsson, A. Berning, P. Celani, D.L. Cooper, M.J.O. Deegan, A.J. Dobbyn, F. Eckert, C. Hampel, G. Hetzer, P.J. Knowles, T. Korona, R. Lindh, A.W. Lloyd, S.J. McNicholas, F.R. Manby, W. Meyer, M.E. Mura, A. Nicklass, P. Palmieri, R. Pitzer, G. Rauhut, M. Schutz, U. Schumann, H. Stoll, A.J. Stone, R. Tarroni, T. Thorsteinsson, H.-J. Werner.
[37] C. Hampel, H.-J. Werner, J. Chem. Phys. 104 (1996) 6286.
[38] E. Papajak, D.G. Truhlar, J. Chem. Theory Comput. 6 (2010) 597.
[39] F.-M. Tao, Y.-K. Pan, J. Chem. Phys. 97 (1992) 4989.
[40] S. Miller, J. Tennyson, B. Follmeg, P. Rosmus, H.J. Werner, J. Chem. Phys. 89 (1988) 2178.
[41] S.F. Boys, F. Bernadi, Mol. Phys. 19 (1970) 553.
[42] F. Lique, A. Spielfieldel, Astron. Astrophys. 462 (2007) 1179.
[43] H.-J. Werner, B. Follmeg, M.H. Alexander, J. Chem. Phys. 89 (1988) 3139.
[44] J.M. Hutson, S. Green, MOLSCAT computer code Vesion 14, United Kingdom 1994, Collaborative Computational Project N.6 of Science Engineering Research Council.
[45] A.M. Arthurs, A. Dalgarno, Proc. R. Soc. London A 256 (1960) 540.
[46] D.E. Manolopoulos, J. Chem. Phys 85 (1986) 6425.
[47] L.N. Smith, D.J. Malik, D. Secrest, J. Chem. Phys. 71 (1979) 4502.
[48] K.M. Christoffel, J.M. Bowman, J. Chem. Phys. 78 (1983) 3952.